Magn Reson Mater Phy (2007) 20: 1–9
DOI 10.1007/s10334-006-0062-y

RESEARCH ARTICLE

**M. Oppitz**
**J. Pintaske**
**R. Kehlbach**
**F. Schick**
**G. Schriek**
**C. Busch**

# Magnetic resonance imaging of iron-oxide labeled SK-Mel 28 human melanoma cells in the chick embryo using a clinical whole body MRI scanner

Received: 3 July 2006
Revised: 10 November 2006
Accepted: 17 November 2006
Published online: 19 December 2006


M. Oppitz (✉) · G. Schriek · C. Busch
Department of Experimental Embryology, Institute of Anatomy, University of Tübingen, Österbergstr. 3, 72074 Tübingen, Germany
E-mail: moppitz@anatom.uni-tuebingen.de

J. Pintaske · R. Kehlbach · F. Schick
Department of Diagnostic Radiology, University Hospital of Tübingen, Tübingen, Germany

**Abstract** *Purpose*: To evaluate advantages and limitations of magnetic resonance imaging (MRI) to monitor the migration of superparamagnetic iron oxide (SPIO) labeled cells in the chick embryo.
*Materials and methods*: Labeled human SK-Mel 28 melanoma cells were injected into the E2 chick embryo neural tube. Embryos were examined with a clinical 3 T MRI whole body system using 3D $T_2^*$-weighted sequences with isotropic spatial resolutions of 0.3–1.0 mm. MR-measurements of embryos were performed 2 – 16 days after cell injection. MRI findings were verified by dissection and histology.
*Results*: After injection, melanoma cells formed aggregations that were detectable in the neural tube as signal voids in MR images from day 2 after injection. Emigrating cells later left MRI detectable tracks. Aggregates that remained in the neural tube left label that was absorbed by glia cells. In E18 chick embryos, signals of haematopoiesis interfered with signals from cell labeling.
*Conclusion*: It was shown that SK-Mel 28 cells will resume the neural crest pathways after injection into the embryonic micro-environment. SPIO cell labeling allows monitoring of transplanted melanoma cells during embryonic development. MRI using the standard clinical equipment promises to be valuable for high-sensitive monitoring of ex-vivo labeled cells in the chick embryo.

**Keywords** SPIO · Cellular imaging · Cell tracking · Chick embryo · SK-Mel 28 · HMB-45

## Introduction

The analogies between embryonic development and malignant transformation of cells have become a fascinating area of research within the last decade [1]. Embryonic traits of highly invasive cancer cells, such as expression of the embryonic transcription factor *Slug* in malignant melanomas, have come into focus as mechanisms that influence cancer progression [2]. The invasive behavior of melanocytes after malignant transformation to melanoma cells has been discussed and attributed to their origin from the embryonic neural crest [2]. As neural crest derivatives, malignantly transformed melanocytes transplanted into their former embryonic micro-environment represent an interesting approach for the understanding of cancer biology. The crucial step for neural crest cell migration is being characterized as epithelial-to-mesenchymal transformation (EMT) [3]. An analogy between active invasive behaviour of cancer cells and EMT has been postulated [4]. By analyzing the pattern of melanoma cell migration in the embryo, it may be possible to determine specific factors involved in malignant invasive growth.

Previous histological studies had shown that human SK-Mel 28 melanoma cells transplanted into the chick

embryo neural tube were able to resume neural crest cell migration. The melanoma cells were detected by immunohistochemistry with HMB-45 monoclonal antibody and in situ hybridization with human specific hALU DNA probe. Neural crest cells were identified in paraffin serial sections by using the neural crest specific marker HNK-1. Although the precursor cells of melanocytes of the skin migrate along the lateral neural crest pathway, the study showed that melanoma cells were also found along the medial pathway [5]. Mouse B16-F1 melanoma cells that were transplanted into the chick neural tube integrated into the neural crest and followed the medial and lateral neural crest pathways by active migration. In addition, invasive growth of melanoma cells was observed after transplantation into ectopic locations, such as the embryonic eye cup (Oppitz et al., in press). Similar fluorescence microscopy observations of melanoma cells in the chick embryo have been reported [6]. However, although some mechanisms that influence emigration of melanocytic precursor cells from the neural crest have been identified, the fate of cells in advanced stages of the chick embryo is not easily predictable, so that further studies are required.

Tracking of cells in the whole embryo by in-situ-hybridization is limited by low signal resolution in whole-mount embryos [7], loss of melanoma antigen induced by immune reaction [8], artifacts caused by fixation, and the time-consuming difficulty of 3D-remodeling from sections. Magnetic resonance microscopy (MRM) has shown to be promising for the anatomical study of mouse embryos [9]. In earlier studies on chick embryos ultra high magnetic fields of 17.6 T and a mixture of gadolinium, albumin and gelatin for fixation were used to obtain satisfactory signal-to-noise ratios [10]. By modifying earlier methods, it has even become feasible to render hollow embryonic organs [11]. Meanwhile, MRM has become an alternative method with high resolution that even allows monitoring the development of the heart of chick embryos [12].

For cell tracking previous studies were dependent on radionuclotide labels such as 111-In. MRM tracking of cells labeled *ex vivo* with superparamagnetic iron nanoparticles (SPIO) has meanwhile been successfully applied in small organisms [13–16]. As far as cellular imaging is concerned, several cell types have successfully been labeled, e.g., macrophages, glioma cells, and oligodendrocyte progenitors (reviewed by [14]). Cell fate in the organism can be monitored by MR imaging without reported major short- nor long-term toxic side effects on non-transformed cells and cancer cells [17,18]. However, SPIO labeling can be associated with toxic effects, such as induction of apoptosis and inhibition of stem cell differentiation, if the cells are incubated at very high iron concentrations (e.g., $\geq$500 $\mu$g Fe/ml [19]). In our recent publication, we were able to show that SPIO-labeling of subventricular neurosphere stem cells neither affects viability nor morphogenetic properties of the cells after transplantation into the neural tube of chick and quail embryos [20]. Other authors have proposed that SPIO labeling of mesenchymal stem cells inhibits chondrogenesis but not adipogenesis or osteogenesis [21].

The objective of this study was to evaluate the advantages and limitations of MRI to monitor the migration of SPIO labeled melanoma cells transplanted into the chick embryo. Moreover, we wanted to extend previously published data [5] by solid data from long-term observations of transplanted melanoma cells in the embryo.

## Materials and methods

### Breeding of chick embryos and experimental procedure

All animal work was performed in accordance with local ethical guidelines. The study was approved by the institutional animal care committee of the University of Tübingen.

Fertilized eggs of white leghorn chicken (*Gallus Gallus domesticus*) were obtained from a local hatchery (Weiss, Kirchberg, Germany) and incubated at 37.8°C and 70% humidity in a brooder (Ehret, Emmendingen, Germany). Embryonic development was verified according to morphologic criteria described by Hamburger and Hamilton (HH) [22]. Eggs were fenestrated after 2 days of incubation (stage 12–13 HH). SK-Mel 28 cells that had been loaded with iron oxide nanoparticles were injected into the neural tube. After injection, eggs were neatly sealed with electrical adhesive tape ("Super33+", 3 M, St Paul, MN) and kept in the brooder for another 2 – 16 days. Before MRI examination, older embryos were anaesthetized by application of 0.5 ml of Ketamine 1:100 on the chorioallantois in order to prevent spontaneous movements of the embryo. The anesthetic was taken up by the chorioallantoic blood and lymph vessels and caused instant reaction. For macroscopical and histological evaluation, the anaesthetized animals were killed by decapitation. During incubation, vitality of the embryos was monitored twice daily by diaphanoscopy. Weak animals (identified by reduced movements in ovo) that probably would not have survived transport and the MRI procedure were anesthetized and examined without delay. In these cases, embryos were removed from the egg and embedded in 1% agar with 10% egg yolk added before MRI. Of a total of 50 embryos, 35 embryos (70%) survived the transplantation procedure and the incubation time. Of these 35 embryos, 28 were scanned alive, while 7 were scanned dead and embedded in agar.

### Loading and injection of SK-Mel 28 cells

Confluent cultures of SK-Mel 28 human melanoma cells (HTB-72, ATCC, Rockville, MD, USA) were loaded with Ferucarbotran (SHU 555A, Resovist®, Schering, Berlin, Germany) by dilution of a sterile solution (28 mg Fe/ml) in cell culture medium (RPMI-1640 (Biochrom, Berlin, Germany); 10% fetal calf serum (Roche, Mannheim, Germany); 2 mmol/l L-glutamine, 100 U/ml Pen-Strep (Roche) and 25 mmol/l HEPES buffer (Biochrom)) to

a final concentration of 200 $\mu$g Fe/ml for 15 h. The concentration of added Ferucarbotran was calculated to a final concentration of 200 $\mu$g Fe/ml culture medium resulting in an entire amount of 1,000 $\mu$g Fe within 5 ml culture medium. For photometric determination of the iron content of the cells a Ferrozine-based spectrophotometric assay (Eisen Ferene S Plus®, Rolf Greiner Biochemica, Flacht, Germany) was used, resulting in an average iron load of 30–60 pg iron per cell. Electron microscopy revealed that iron particles were stored both intracellularly and on the cell's surface. Cellular viability after the incubation was examined by using CASY®2 (CASY®2 Cell Counter and Analyzer System, Model TT, Schärfe System, Reutlingen, Germany) according to the ECE-method described by Lindl et al. [23]. We saw no difference in viability of control cells and labeled cells. About $5 \times 10^5$ Ferucarbotran labeled melanoma cells were injected into the neural tube of chick embryos stage 12–13 (HH) via a mouth pipette equipped with a pointed borosilicate glass capillary (World Precision Instruments, Sarasota, USA). Fifty embryos in six different experiments received Ferucarbotran labeled SK-Mel 28 cells. Embryos in each experiment were kept in the incubator for defined time points: 2, 4, 14, or 16 days. At the end of the incubation period, MR imaging was done, followed by anatomical and histological examination.

### Magnetic resonance microscopy

In a period ranging from 2 to 16 days incubation time after cell injection (total incubation times: 4 ($n = 13$), 7($n = 10$), 16($n = 7$), and 18 days ($n = 5$); chick hatching usually occurs on day 21), the embryos underwent the MR examination. Due to the small size of the E2 embryo, no embryos were scanned before or directly after melanoma cell injection. MR imaging of the eggs inevitably leads to a delay in the development or even to death of the embryo, caused by transport stress, inadequate temperature and humidity, and damage by vibration during scanning time. We therefore, scanned each embryo at just one specific time point as mentioned above. Four to six embryos were scanned on seven different days. As control two embryos without cell injection were scanned at E16, and two at E18. Due to the lack of endogenous iron in E4 and E6 chick embryos, we did not conduct control experiments for E4, and only one for E6. MR imaging was performed using a clinical MR whole-body scanner operating at 3 T (Magnetom Trio, Siemens Medical Solutions, Erlangen, Germany). Eggs or agar-embedded embryos were placed in a wrist coil (Siemens). An orthogonal multislice sequence localizer was run for determination of position and selection of the desired region. Then, 3D data sets covering the whole body of the embryo were recorded using a fast low angle shot (FLASH) gradient echo sequence. Gradient echo sequences are known to be most sensitive to any kinds of magnetic field inhomogeneities, such as those due to magnetically labeled cells [24]. Aggregations of labeled cells were reflected either as low intensity signal spots or signal voids, particularly in $T_2^*$ weighted gradient echo MRI. The echo time (TE) was varied between 6 and 20 ms. The isotropic spatial resolution was varied between 0.3 and 1.0 mm length of the volume elements. The other sequence parameters were repetition time (TR) 30 ms, 1 averages, 80 slices per slab, Field-of-View (FoV) 128 × 128 mm$^2$, flip angle 20°. In order to achieve an isotropic spatial distribution of 0.3 mm voxel length, the matrix size was 384 × 384 and the measurement time was about 12 s per slice.

### Processing of embryos, slicing, and macroscopical staining of iron deposits

After MRI, embryos were harvested by opening the egg, excision of the amnion with a fine pair of scissors, and fine preparation in a glass filled with Tyrode's solution. Before excision, embryos were again anaesthetized with Ketamine, and subsequently killed by decapitation. The excised embryos were fixed overnight at 4°C in 4% para-formaldehyde in 0.1 m PBS. The whole embryos were cut into longitudinal or transversal slices using fine forceps and scalpels. Sections were stained for ferric iron using the Prussian blue reaction. The stained sections were embedded in Kaiser's glycerol gelatin (Merck, Darmstadt, Germany) in a plastic Petri dish, and photos were taken using a binocular microscope (Zeiss, Göttingen, Germany) with a stereo camera attached.

### Histochemical detection of iron

Four E4 and two E18 embryos were dehydrated with ethanol, treated with xylene and embedded in Paraplast. Serial sections (5 $\mu$m thick) were mounted on polylysin-coated slides. After deparaffinization and rehydration, sections were stained with standard Prussian blue reagent and heated with a microwave oven for 30s. Staining was continued for 5 min. Nuclei were counterstained with acidified hematoxylin. Stained sections were dehydrated and embedded in DEPEX (BDH, Poole, UK) before microscopy.

### Immunohistochemistry for melanoma cells

For detection of mouse melanoma cells HMB-45 (Dako, Hamburg, Germany) 1:200 was used overnight at 4°C after antigen retrieval with target retrieval solution (high pH, 1:10; Dako) at 37°C for 30 min. Goat anti-mouse IgG – biotin conjugate 1:250 (Linaris, Wertheim, Germany) was applied at room temperature for 1 h, binding to biotin-streptavidin-HRP complex 1:150 and development of red HRP-substrate (Vector Laboratories, Burlingame, CA, USA) for 1 h.

## Results

Following the injection of SPIO-labeled melanoma cells (as depicted in Fig. 1) on E2, 70% of embryos (35/50) survived until the fixed time point of MRI. The rate of survival was slightly lower for the embryos that were kept for long period of time after injection. In a period ranging from 2 to 16 days incubation time after cell injection [total incubation time: 4 ($n = 13$), 7 ($n = 10$), 16 ($n = 7$), and 18 days ($n = 5$)], the embryos underwent the MR examination. In all surviving embryos

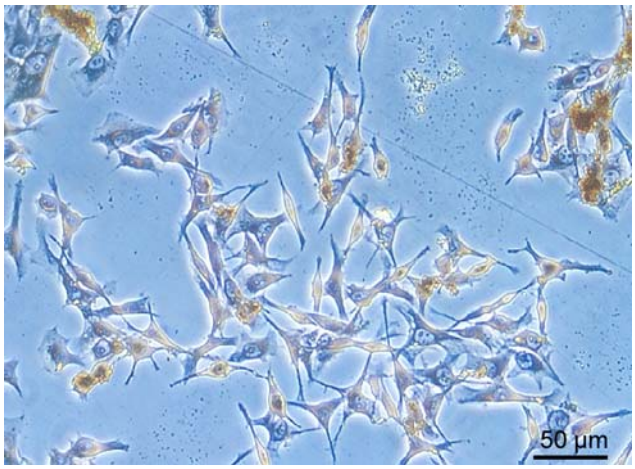


**Fig. 1** SK-Mel 28 cells 24 h after the labeling procedure, phase contrast image. Iron deposits appear as brown cytoplasmatic spots and crystalline structures on cell surface

with short interval of observation (2 days after injection, see Fig. 2a for comparison), SPIO induced signal voids were observed (Fig. 2b). Immunostaining of SK-Mel 28 cells with HMB-45 (Fig. 2c) and histology with Prussian blue staining (Fig. 2d) documented that integration of injected cells had occurred at this stage (23 (HH)). Prussian blue staining in parallel sections indicated tracks of iron from emigrating cells that reached from the embryonic roof plate to the area lateral of the myotome. This corresponds to the lateral pathway of emigrating neural crest cells. Prussian blue staining did not clarify whether extracellular or intracellular labeling on the injected cells had occurred. Electron microscopy of loaded SK-Mel 28 demonstrated that both were true (not shown). As Fig. 2c demonstrates, iron on the surface of SK-Mel 28 is taken up by host cells (bold arrow).

4 days after injection (stage 28 HH) detailed imaging of the embryo was feasible. Embryos without melanoma cell injection showed no detectable signal voids (Fig. 2e). Injected embryos showed signal voids in the dorsal region of the embryo at regular intervals (Fig. 2f, arrows). Whole mount staining of the embryo confirmed an identical pattern of iron deposits in the neural tube (Fig. 2g). Histology (not shown) demonstrated that the cells were partially integrated into the host neural crest, while non-integrated cells remained in the neural tube lumen.

The MR image of the segmentation in an E16 chick embryo (14 days after injection) is shown in Fig. 3. In accordance with our immunohistochemical findings, aggregates of iron-loaded SK-Mel 28 cells were detectable in $T_2^*$ weighted MR images (Fig. 3a, c). Embryos at this advanced stage of development showed highly contrasted iron deposits in the spinal chord and brain (Fig. 3b). The MRI findings were verified in the embryos by dissection and iron staining. Iron deposits from SPIO were found in lateral parts of the cervical region of the embryo, and in the spinal chord. Aside from spots of low signal density in the region of the spinal cord that were stained with Prussian blue, dissection revealed additional irregular formations that were negative for iron and contained melanin, thus indicating remnants of SK-Mel28 cells (Fig. 3d). A control embryo MRI (E16) without cell transplantation is depicted in Fig. 3e. No signal voids are detectable.

A representative image of an embryo at E18 (3 days before hatching) is depicted in Fig. 4. The normal organ structures such as spinal column, heart, liver, lung and brain, were clearly distinguishable (Fig. 4a middle image). Signal voids from remnants inside the former neural tube were detected in the trunk and the neck region. One embryo of this experiment is shown where the typical segmental arrangement of low density signal voids outside the spinal chord was demonstrated (Fig. 4a upper and middle image, 4b). Histology of this area revealed deposits of iron in the epidermis (not shown). In the spinal cord, no HMB-45 positive cells were found in the whole series of sections. However, deposits of iron were encountered in the white matter of the spinal chord, surrounded by glial cells (Fig. 4c). In the skeleton, signal voids were especially found in the upper palate bone of the embryo, the vertebrae and in cartilaginous structures of the wing bud (Fig. 4a lower image, 4b). Corresponding staining for iron with strong intensity was found in the prospective bones of the chick, such as ribs and vertebrae (Fig. 4d). In embryos at E18, signal intensities were highly contrasted and made imaging of deposits from SPIO impossible due to endogenous accumulation of iron necessary for haematopoiesis. There was no detectable difference of iron in the bone marrow of embryos that received iron-loaded melanoma cells compared to the group of non-injected embryos. As a control, the oldest embryo (E18) was imaged at 1.5 T without showing major differences in image information (Fig. 4e).

## Discussion

SPIO-labelled melanoma cells had been injected into the neural tube of chick embryos. The results show that sufficient cell labeling was achieved for the detection of SPIO-labeled melanoma cells in E4 chick embryos with the critical length of 15 mm. To our knowledge, this is the first report of cellular tracking in the chick embryo using clinical MRI equipment under the conditions described above. In embryos younger than E4 no sufficient spatial resolution of the images combined with a reasonable signal-to-noise ratio was achievable with the present

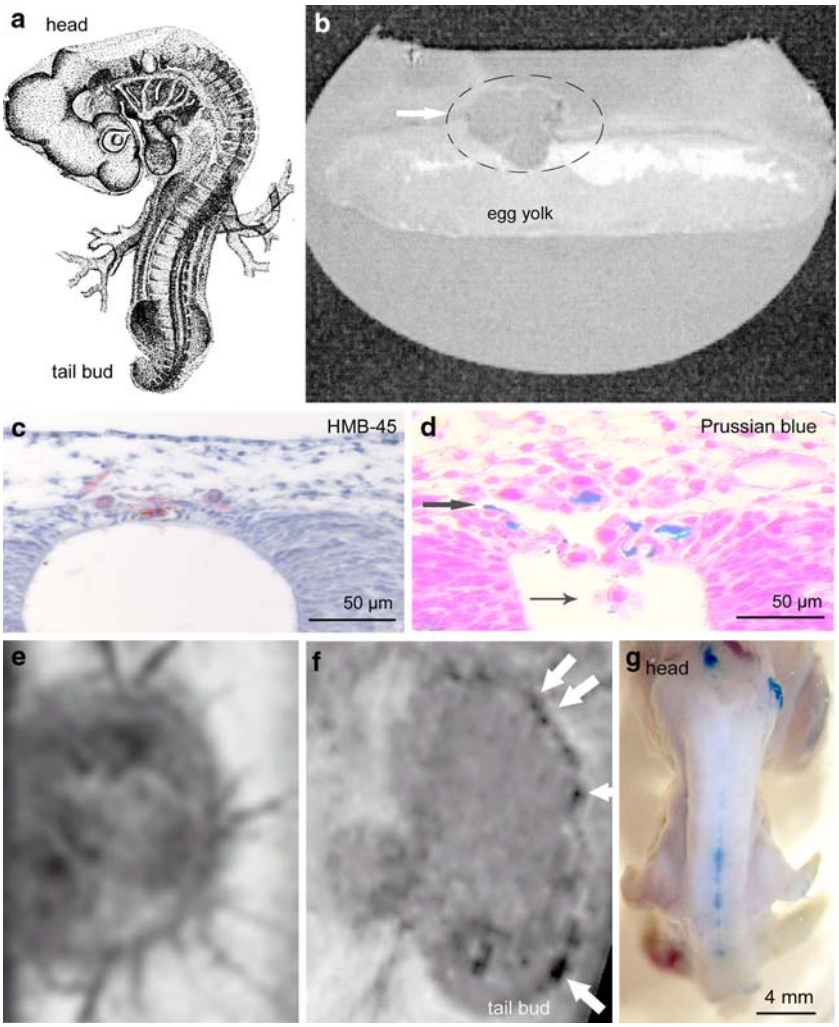


**Fig. 2** Observations in early stages of the chick embryo. **a** Schematic sketch of E4 chick embryo (from (29)). **b** Formation of aggregates in chick embryo stage 23 (HH), total incubation time 4 days, 2 days after injection of SPIO-labeled SK-Mel 28 cells. Formation of aggregates visualized by 3 T MRI. Arrow marks signal voids in the chick embryo in the windowed egg. The window in the egg shell is visualised as a flat shape of the upper part of the egg. **c** Histology of embryo shown in **b**. Labeling with HMB-45 (red adduct) demonstrates emigrating melanoma cells. **d** Same embryo. Parallel section stained with Prussian blue reaction. SK-Mel 28 cells can be identified by their size. Melanoma cells without label are visible, together with labeled cells (*slim arrow*) and presumed iron deposited in the embryo (*bold arrow*). Optical microscopy gives no final decision about intra- or extracellular labeling of the cells. **e** MR imaging of E6 chick embryo without melanoma cell transplantation (control). **f** MR imaging of injected E6 (6 days old, 4 days after injection) chick embryo with signal voids from segmental aggregates of SK-Mel 28 (*white arrows*). **g** Whole mount of same embryo as in **d**, rear view; Prussian blue reaction product stains iron deposits

experimental set-up. In later stages, we regularly observed the formation of SPIO-loaded cellular aggregates in the area of the neural tube. This pattern (formation of segmentally arranged aggregates at the level of intersomitic clefts due to longitudinal migration of cells in the neural tube) also occurred in earlier studies with labeled and unlabeled SK-Mel 28 cells [5].

It is yet unclear how this regularly observed pattern is connected to the emigration of the melanoma cells. The observation of signals of aggregates of SPIO-labeled SK-Mel 28 cells confirms our earlier histological observations that were reported on chick embryos that were injected with unlabeled melanoma cells [5]. During melanoma cell migration, extracellular label is taken up by embryonic tissue. As melanoma cells that have left the roof plate undergo apoptosis on their migration to the para-aortic ganglia (Oppitz et al., Melanoma Research, in press), it can be concluded that iron from apoptotic melanoma cells was also absorbed. Due to apoptosis of melanoma cells in the neural crest pathways, no formation of

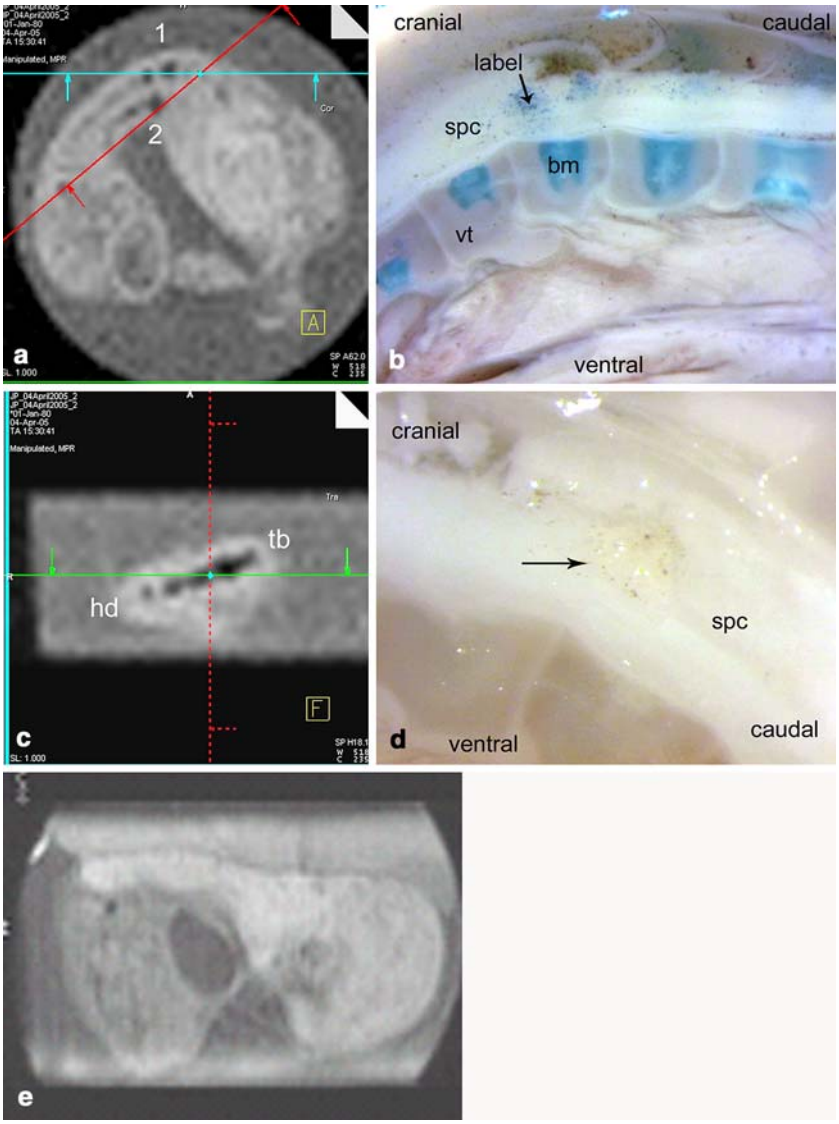


**Fig. 3** MRI and histochemical in situ detection of iron accumulation in the E16 chick embryo (14 days after injection). **a** Whole-body image of E16 chick embryo. Contrast-rich patches show segmental iron deposits ("1") and signal voids of bone marrow in vertebrae ("2"). **b** Same embryo, sagittally cut section of neck region. Prussian blue makes iron deposit in the spinal chord (*arrow*). *spc* spinal chord, *vt* vertebra, *bm* bone marrow. **c** MR imaging of segmentally arranged aggregates of cells, rear view of **a** *hd* head, *tb* tail bud. **d** Close-up view of iron-free remains of SK-Mel 28 cells in longitudinal section of spinal chord, visible by melanin granules (*arrow*). *spc* spinal chord. **e** NMR imaging of control E16 chick embryo, for comparison

malignant tumors was observed that would have resulted in reduced overall survival rate of embryos. We have demonstrated that the survival rate of embryos with melanoma cell injected into the neural tube did not differ from the survival rate of untreated embryos in windowed eggs (Oppitz et al., Melanoma Research, in press). Moreover, this study shows that labeling of injected melanoma with Ferucarbotran did not influence the outcome of the experiment.

Embryos were found to be optimal for observing iron deposits caused by migration of SK-Mel 28 cells 14 days after injection (E16) with the technique described above. Unspecific signal intensity in the liver and bones was comparatively low at this stage. From E18 onwards, intense signal voids in bony structures and the liver increasingly impaired MR imaging. We attribute this to enrichment of iron caused by haematopoiesis that reaches its peak activity in the hepato-lienal compartment between E14

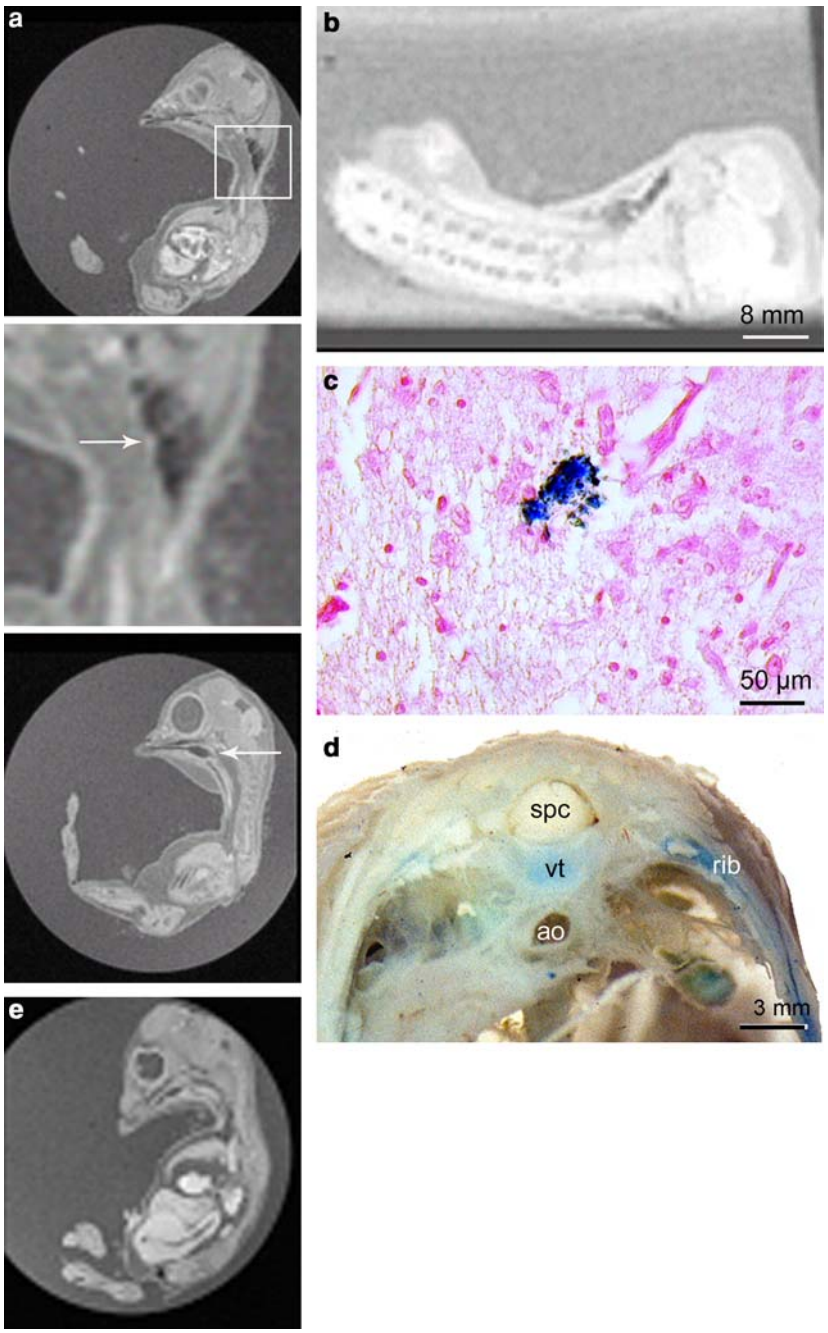


**Fig. 4** MRI and histochemical detection of iron accumulation in the E18 chick embryo. **a** *Upper image* Plane of section close to the sagittal plain. Heart and liver are visible. Signal voids from iron deposits in the cervical region are observed. *Frame* indicates middle image. *Middle image* Blow up view of segmental signal voids outside the spinal chord (*arrow*). *Lower image* Reconstructed parasagittal section of embryo. Signal void in the lower palate (*arrow*) indicates beginning signal from bony structures and was also found in control embryos. **b** Same embryo, rear view. Signal voids outside of the spinal cord appear in the cervical region. **c** Prussian blue reaction of iron deposit in the spinal cord at high magnification. **d** Blue reaction product of Prussian blue staining in transversally cut embryo. *spc* spinal chord, *vt* vertebra, *ao* aorta. **e** MRI of embryo (E 18) without cell injection

and E19, and the subsequent onset of hematopoiesis in the bone marrow [25].

The result of our technical procedure corresponds to results from experiments in other animal systems. Using Prussian blue reaction and MRI, we found a correlation between reaction product and contrast-rich deposits in the adult mouse heart of $T_1$-weighted images [27]. In contrast to our study, SPIO labeled embryonic stem cells were

injected in the heart muscle and were observed at the spot of injection. Experimental high magnetic fields of 4.7 T and a 35 mm birdcage coil were required.

Our results show that transplanted cells labeled with contrast agents such as Ferucarbotran can be tracked down in the chick embryo model. Other options for cell labeling in this particular animal model comprise vital staining (e.g., DiI), or transfection of cells with green fluorescent protein (GFP). GFP fluorescence on a cellular level can be monitored successfully as long as cells emigrate on superficial pathways [20]. The visibility of GFP fluorescence labeled cells is limited by the increasing size of the developing embryo. Vital dyes only allow a relatively short period of observation. Adult enteric neural stem cells stained with DiI that had been transplanted as neurospheres into the lower appendages of the 3 day chick embryo could only be followed by live fluorescence for a maximum of 3 days following transplantation (own observations, manuscript in preparation). Therefore, SPIO labeling offers a satisfactory alternative. However, the study also demonstrates that the SPIO label has its limitations due to signal voids originating from the bone marrow. A fundamental drawback of those negative contrast agents is that the agent cannot be distinguished from signal voids in the image reflecting areas of low proton density. Various other sources of hypointensities can be present, or the magnetic field background can be inhomogeneous in MR images. Due to the negative contrast, it is often difficult to accurately determine the presence of magnetically labeled entities under in vivo conditions, and the differentiation of iron labeled cells and an inherent tissue structure is often problematic. An alternative way for further studies would be the use of positive NMR contrast media that are less sensitive to confounding signals from the bone marrow. Positive contrast media have been successfully applied by Bulte et al. [14], who used mouse embryonic stem cells that had been differentiated into the neural lineage with retinoic acid, containing 9–14 pg of iron per cell after labeling with magnetodendrimers MD-100. It was shown that these cells could be tracked after transplantation into the spinal cord of rats receiving contusion injury (reviewed by [14]).

It has to be taken into consideration that labeling cells with contrast agents results in a broad range of iron yields. The relatively high iron content of the SK-Mel 28 cells used in our experiments was verified in seven independent repetitions. This underlines that for every system investigated — different cell types, contrast agents and eventually used transfection agents — the conditions have to be evaluated carefully and the results may differ strongly.

Another drawback was the lack of sensitivity of the described MRI procedure that did not detect single emigrating cells that were visualized in histological sections. It should be noted that the MR image signal void does not directly reflect the location and spatial distribution of the iron oxide nanoparticles. Theoretical and experimental studies of the complex effects involved can be found in the papers include in the reference list [24, 26].

The study was further limited by the need to sacrifice animals after performing MRI. As pointed out, MR imaging of the eggs inevitably leads to delay in development or even death of the embryo, caused by transport stress, inadequate temperature and humidity, and damage by vibration during scanning time. Therefore, serial imaging of the same embryo was not feasible. Clinical MRI often does not permit an optimum experimental setup including minimum requirements of transport and optimum breeding conditions during MRI. The use of experimental animal scanners is a way to overcome these limitations in future studies.

In conclusion, MRI tracking of injected SK-Mel 28 cells with SPIO confirmed the results from our earlier studies, and demonstrated emigration of the transplanted melanoma cells on neural crest cell pathways, without developing malignant tumors. The MRI detection of SPIO labeled cells is a promising approach for understanding the migration pathways of cells after transplantation or injection into animals. Although high resolution and high field MRI is advantageous in detecting labeled cells [27], the present study demonstrates that cell migration can be visualized using clinical MRI equipment even in the chick embryo. Similar conclusions were found for SPIO-labeled haematopoietic stem cells injected in the circulatory system of the mouse, which have successfully been traced using 1.5 T MR equipment [28]. In addition, it opens a new perspective for cancer therapy, in which cancer cells and metastases could be labeled and localized in the organism in a similar manner to optimize radiation therapy. Another field of research for MRI imaging is visualizing transplanted cells in experimental diseases of the central nervous system (CNS). There has been a broad range of suggestions for application of MRI in experimental studies (reviewed by [14]).

## Conclusions

MRI cell tracking is a useful tool for confirming the emigration pattern of transplanted melanoma cells loaded with SPIOs in a small embryo. The value of MRI is based on its non-invasive and non-deleterious nature that allows the complementary use of whole mount staining and histological techniques.

**Acknowledgements** The authors thank Prof. Dr. Ulrich Drews for his support of the study, and Philip Specht, PhD for critical reading of the manuscript. We thank Ingrid Epple for preparing paraffin sections, and Leokadia Macher for the immunohistochemistry.

## References


1. Noda S, Lammerding-Koppel M, Oettling G, Drews U (1998) Characterization of muscarinic receptors in the human melanoma cell line SK-Mel-28 via calcium mobilization. Cancer Lett 133:107–114
2. Gupta PB, Kuperwasser C, Brunet JP, Ramaswamy S, Kuo WL, Gray JW, Naber SP, Weinberg RL (2005) The melanocyte differentiation program predisposes to metastasis after neoplastic transformation. Nature Genetics 37:1047–1054
3. Hay ED (2005) The mesenchymal cell, its role in the embryo, and the remarkable signaling mechanisms that create it. Dev Dyn 233:706–720
4. Kuphal S, Bosserhoff AK (2006) Influence of the cytoplasmatic domain of E-cadherin on endogenous N-cadherin expression in malignant melanoma. Oncogene 25:248–259
5. Schriek G, Oppitz M, Busch C, Just L, Drews U (2005) Human SK-Mel 28 melanoma cells resume neural crest cell migration after transplantation into the chick embryo. Melanoma Res 15:225–235
6. Kulesa PM, Kasemeier-Kulesa JC, Teddy JM, Mararyan NV, Seftor EA, Seftor REB, Hendrix MJC (2006) Reprogramming metastatic melanoma cells to assume a neural cell-like phenotype in an embryonic microenvironment. Proc Natl Acad Sci USA 103:3752–3757
7. Lopez-Sanchez C, Puelles L, Garcia-Martinez V, Rodriguez-Gallardo L (2005) Morphological and molecular analysis of the early developing chick requires an expanded series of primitive streak stages. J Morphol 264:105–116
8. Marincola FM, Hijazi YM, Fetsch P, Salgaller ML, Rivoltini L, Cormier J, Simonis TB, Duray PH, Herlyn M, Kawakami Y, Rosenberg SA (1996) Analysis of expression of the melanoma-associated antigens MART-1 and gp100 in metastatic melanoma cell lines and in in situ lesions. J Immunother Emphasis Tumor Immunol 19:192–205
9. Smith BR, Johnson GA, Gronman EV, Linney E (1994) Magnetic resonance microscopy of mouse embryos. Proc Natl Acad Sci USA 91:3530–3533
10. Hogers B, Gross D, Lehmann V, de Groot HJM, de Roos A, Gittenberger-de Groot AC, Poelmann RE (2001) Magnetic resonance microscopy at 17.6-Tesla on chicken embryos in vitro. J Magn Res Imaging 14:83–86
11. Zhang X, Yelbuz TM, Cofer GP, Choma MA, Kirby ML, Allan Johnson G (2003) Improved preparation of chick embryonic samples for magnetic resonance microscopy. Magn Res Med 49:1192–1195
12. Yelbuz TM, Wessel A, Kirby ML (2004) (Studies on morphogenesis and visualization of the early embryonic heart with regard to development of conotruncal heart defects) Studien zur Morphogenese und Visualisierung des frühen embryonalen Herzens im Hinblick auf die Entwicklung konotrunkaler Herzfehler. Z Kardiol 93:583–594
13. Daldrup-Link HE, Rudelius M, Metz S, Bräuer R, Debus G, Corot C, Schlegel J, Link TM, Peschel C, Rummeny EJ, Oostendorp RA (2005) Migration of iron oxide-labeled hematopoetic progenitor cells in a mouse model: in vivo monitoring with 1,5-T MR imaging equipment. Radiology 234:197–205
14. Bulte JWM, Kraitchman DL (2004) Iron oxide MR contrast agents for molecular and cellular imaging. NMR Biomed 17:484–499
15. Frank JA, Anderson SA, Kalsih H, Jordan EK, Lewis BK, Yocum GT, Arbab AS (2004) Methods for magnetically labeling stem and other cells for detection by in vivo magnetic resonance imaging. Cytotherapy 6:621–625
16. Weissleder R, Mahmood U (2001) Molecular imaging. Radiology 219:316–333
17. Arbab AS, Bashaw LA, Miller BR, Jordan EK, Lewis BK, Kalish H, Frank JA (2003) Characterization of biophysical and metabolic properties of cells labeled with supramagnetic iron oxide nanoparticles and transfection agent for cellular MR imaging. Radiology 229:838–846
18. Arbab AS, Bashaw LA, Miller BR, Jordan EK, Bulte JW, Frank JA (2003) Intracytoplasmic tagging of cells with ferumoxides and transfection agent for cellular magnetic resonance imaging after cell transplantation: methods and techniques. Transplantation 76:1123–1130
19. Metz S, Bonaterra G, Rudelius M, Settles M, Rummeny EJ, Daldrup-Link HE (2004) Capacity of human monocytes to phagocytose approved iron oxide MR contrast agents in vivo. Eur Radiol 14:1851–1858
20. Busch C, Oppitz M, Sailer MH, Just L, Metzger M, Drews U (2006) BMP-2 dependent integration of mouse adult subventricular stem cells into the neural crest of chick and quail embryos. J Cell Sci 119:4467–4474
21. Kostura L, Kraitchmann DL, Mackay AM, Pittenger MF, Bulte JWM (2004) Feridex labeling of mesenchymal stem cells inhibits chondrogenesis but not adipogenesis or osteogenesis. NMR Biomed 17:513–517
22. Hamburger V, Hamilton HL (1992) A series of normal stages in the development of the chick embryo. Dev Dyn 195:231–272
23. Lindl T, Lewandowski B, Sheyrogg S, Staudte A (2005) An evaluation of the in vitro cytotoxicities of 50 chemicals by using an electrical current exclusion method versus the neutral red uptake and MTT assays. Altern Lab Anim 33:591–601
24. Pintaske J, Helms G, Bantleon R, Kehlbach R, Wiskirchen J, Claussen CD, Schick F (2005) (A preparation technique for quantitative investigation of SPIO-containing solutions and SPIO-labeled cells by MRI). Methode zur quantitativen Messung von SPIO-haltigen Flüssigkeiten und Zellen mit MRI. Biomed Tech (Berl) 50:174–180
25. Wong GK, Cavy MJ (1993) Development of the liver in the chicken embryo. II.Erythropoetic and granulopoetic cells Anat Rec 235:131–143
26. Pintaske J, Müller-Bierl B, Schick F (2006) Geometry and extension of signal voids in MR images induced by aggregations of magnetically labelled cells. Phys Med Biol 51:4707–4718
27. Himes N, Min J-Y, Lee R, Brown C, Shea J, Huang X, Xiao Y-F, Morgan JP, Burstein D, Oettgen P (2004) In Vivo MRI of embryonic stem cells in a mouse model of myocardial infarction. Magn Res Med 52:1214–1219
28. Niemann BJ, Bock NA, Bishop J, Sled JG, Chen J, Henkelmann M (2005) Fast spin-echo for multiple mouse magnetic resonance phenotyping. Magn Res Med 54:532–537
29. Patten BM (1948) The early embryology of the chick. The Blakiston Co, Philadelphia